Catalysis Today 175 (2011) 338–345

Contents lists available at ScienceDirect

Catalysis Today

journal homepage: www.elsevier.com/locate/cattod

Comparative studies of silver based catalysts supported on different supports for the oxidation of formaldehyde

Dan Chen[a], Zhenping Qu[a,*], Shijin Shen[a], Xinyong Li[a], Yong Shi[a], Yi Wang[a], Qiang Fu[b], Jingjing Wu[b]

[a] Key Laboratory of Industrial Ecology and Environmental Engineering (MOE), School of Environmental Science and Technology, Dalian University of Technology, Dalian, Linggong 116024, China
[b] State Key Laboratory of Catalysis, Dalian Institute of Chemical Physics, Chinese Academy of Sciences, Dalian 116023, China

ARTICLE INFO

Article history:
Received 15 October 2010
Received in revised form 21 February 2011
Accepted 30 March 2011
Available online 4 May 2011

Keywords:
Support
Ag based catalysts
Formaldehyde
TPD
TPSR

ABSTRACT

Temperature programmed desorption (TPD) and temperature programmed surface reaction (TPSR) were employed to study the HCHO adsorption–desorption and the surface reaction on Ag based catalysts supported on different supports (MCM-41, SBA-15, NaY, SiO_2 and TiO_2). According to the analysis of XRD, UV–Vis and H_2-TPR for the as-prepared catalysts, there are four kinds of silver species on the supports, including metallic Ag particles (Ag^0) with subsurface oxygen species, isolated Ag^+ ions, well dispersed Ag_2O and $Ag_n^{\delta+}$ clusters. Moreover, the states, the dispersion and the amount of these silver species seem to be obviously different on different supports. No activity for HCHO oxidation is observed on any supports, and silver particles with some oxygen in bulk were more active for the adsorption and activation of HCHO. MCM-41 and SiO_2 supported silver catalysts give new adsorption sites for HCHO, and it is easily activated at lower temperatures and shows better surface reaction activity for HCHO oxidation. The desorption temperature for HCHO over SBA-15 and NaY supported silver catalysts is relatively higher, and its reaction performance is worse. However no surface reaction is observed on Ag/TiO_2 catalyst during experiments. It is also found that HCHO molecular adsorbed on silver sites could be was oxidized into dioxymethylene (DOM) and formate surface species, and they reacts with oxygen to form CO_2 during TPSR. The activities of different silver based catalysts for HCHO oxidation were closely related to their abilities for the formation of DOM and formate species.

1. Introduction

HCHO is known to cause nasal tumors, irritation of the mucous membranes of the eyes and respiratory tract, and skin irritation in the most volatile organic compounds (VOCs). Many techniques have been developed to eliminate HCHO in the last decades [1–4]. As we all know the catalytic oxidation is widely used in the chemical industry and environmental protection, and the conversion of VOCs into CO_2 and H_2O using heterogeneous catalysts by catalytic oxidation at much lower temperature has proven to be an efficient and practical technology for controlling VOCs emission [5–11]. As a consequence, the formaldehyde catalytic oxidation has been studied over many catalysts [12–18]. Noble metal catalysts (Pt, Pd, Au etc.) possess high activity for the oxidation of HCHO at a low temperature [12,14,19]. However, these catalysts are uneconomical for wide application due to their high costs. Silver has rarely been considered as the catalyst for HCHO oxidation although it has been recognized to show a high activity in several partial oxidation reactions, such as hydrogenation of unsaturated aldehydes [20], partial oxidation of methanol to formaldehyde [21], and oxidative coupling of methane to ethane and ethylene [22], CO oxidation [23,24] and so on. Only relatively low activity for HCHO oxidation was observed on silver supported on MnO_x–CeO_2 and SiO_2 [4,17,18], moreover no investigations about the interaction of reactants with the surface of active sites and the surface reaction process were reported.

Usually pure support has no catalytic activity for most reactions due to the absence of the active sites, and therefore different active metals or metal oxides have been tried to introduce into zeolites and oxides supports. It is well known that the support is the vital factor which affects the formation, the distribution and the dispersion of active species in catalytic oxidation and thus many Refs. [25–27] have been paid to develop catalytic materials and improve their catalytic performance. In review on the support role on the HCHO oxidation, it is suggested that different support results in different catalytic active phases which are related to different

* Corresponding author. Tel.: +86 15542663636.
E-mail addresses: zhenpq@yahoo.com, zhenpq@dicp.ac.cn (Z. Qu).

0920-5861/$ – see front matter © 2011 Elsevier B.V. All rights reserved.
doi:10.1016/j.cattod.2011.03.059

reaction activity. The PtO_xCl active species were formed on the MnO_x–CeO_2 supported Pt, and 100% conversion of formaldehyde could be achieved at ambient temperature in 30 ppm HCHO concentration [15]. The highly dispersed active platinum species in TiO_2 carrier could completely oxidize HCHO at 20 °C [16]. After Pt loading, the OMS-2 catalyst showed a very strong and broad H_2-consumption peak at a maximum of 190 °C, which was attributed to the reduction of PtO_x and partial reduction of MnO_2 [28], and 100% conversion of formaldehyde could only be achieved at 120 °C in 500 ppm HCHO. It has also been found that the highly dispersed and poorly crystallized metallic gold and small amount of oxidized gold in the CeO_2 support catalysts exhibited superior activity for HCHO oxidation at temperatures close to 100 °C [14]. However Fe–O supported Au catalyst gave different gold active sites and activity [29]. Thus it was clearly exhibited that the support showed a strong influence on the nature of the active species and its catalytic activity.

In fact, porous materials with a high surfaces area and a large pore diameter are often used as the catalyst support to disperse active phase with more active sites. Moreover, the porous structure allows the VOC molecules to reach the inner active sites to be readily oxidized. It is well known that mesoporous materials, such as MCM-41 and SBA-15, have very high surface areas and uniform pore diameter (2.0–10.0 nm), which are good for uniformly loading the catalytic active component and consequent catalytic reactions [26,27,30,31]. However, the systematic studies on the effect of the different supports on the nature of active sites and catalytic activity have seldom been reported on the Ag based catalysts for HCHO oxidation.

In view of the investigation of the formaldehyde catalytic oxidation, most attention is focused on the catalytic activity in the fixed bed at present, and many techniques (XRD, XPS, EXAFS, EPR and FTIR spectroscopy) have been employed for its characterization. However, temperature programmed techniques, such as temperature programmed desorption (TPD) and temperature programmed surface reaction (TPSR), have been less often used to study the characteristics of HCHO adsorption–desorption and surface reaction on the catalysts, especially on the silver catalyst. Generally speaking, the recycle catalytic oxidation process comprises diffusion, chemical adsorption, surface reaction, desorption and reverse diffusion steps. The adsorption of the reactant molecular on the active sites plays a key role in the activation of reactant molecular. Thus, it is very significance for investigation about reactant molecular adsorption on the catalyst surface to elucidate its interaction between reactant molecular and catalyst surface and its activity. This adsorption–desorption process and surface reaction can be studied by temperature programmed (TP) techniques, which can probe different surface structures by monitoring the desorbed species over the range of temperature of interest to catalysis [32,33].

In all, the present paper summarizes the results of a more completely comparative study of the adsorption and oxidation of formaldehyde on silver based catalysts supported on different oxide and zeolites surfaces (silica, titania, NaY, MCM-41, SBA-15 zeolites) by using temperature programmed desorption (TPD) and temperature programmed surface reaction (TPSR) and in situ FTIR techniques with the aim to gain new insights as complete as possible of the adsorption and behavior of surface reaction for formaldehyde oxidation on these catalysts, and the knowledge about the effect of the supports and the active silver phase. To obtain information on the adsorption sites and adsorption capacity over the different catalysts, HCHO–TPD is used to study adsorption/desorption behavior. The prepared catalysts are characterized by XRD, N_2 adsorption/desorption, TEM, UV–Vis, H_2-TPR techniques, and their behavior of the surface reaction for HCHO oxidation are investigated in a continuous flow fixed bed reactor by TPSR.

2. Experimental

2.1. Catalyst preparation

Commercial porous materials and metal oxides of different pore structures (MCM-41, SBA-15, NaY, SiO_2 and TiO_2) were used as the supports. To endow the catalytic activity, 8 wt% silver was introduced into these supports using nitrate precursor of silver. The silver catalysts supported on different support (8Ag/M, M: different supports) were prepared by incipient-wetness impregnation method. The wet samples obtained were dried at room temperature and then at 100 °C overnight. The catalysts were sieved into 20–40 mesh granule and then pretreated in flowing O_2/Ar (30 vol.% O_2, 50 ml/min) at 500 °C for 2 h before testing.

2.2. Catalyst characterization

Specific areas were computed from these isotherms by applying the Brunauer–Emmett–Teller (BET) method in Quantachrom NOVA4200e. Before measurement, the samples were treated by degassing at 300 °C for 4 h. The pore diameter distributions were calculated from desorption branches using the BJH (Barrett–Joyner–Halenda) methods.

Powder X-ray diffraction (XRD) measurements of the catalysts were carried out on a Rigaku D/max-γb (λ = 0.1542 nm) and operating at 40 kV and 200 mA. The patterns were taken over the 2θ range from 10° to 80° and a position-sensitive detector using a step size of 0.02°.

Transmission electron microscopy (Tecnai G^2 Spirit) operated at 120 kV was used to study the morphology and the particle size of catalyst samples. The sample was supported on a copper mesh for the TEM analysis.

UV–Vis diffuse reflectance spectra were recorded in air on a SHIMADZU UV–2450 UV-Vis spectrophotometer. Reference spectra were collected with pressed $BaSO_4$ disks. The following parameters were used to collect data: 5.0 spectra band width, 0.5 nm data pitch, 800–190 nm measurement range, and 200 nm/min scanning speed.

H_2-TPR (temperature programmed reduction) was carried out in Quantachrom Automated Chemisorption Analyzer. A 0.1 g sample was pretreated in O_2/Ar (30 vol.% O_2) at 500 °C for 2 h, cooled to room temperature in flow of Ar in a fixed bed reactor. For H_2-TPR study, it was exposed to a flow of 30 ml/min H_2/Ar (10 vol.% H_2) mixture. The temperature was programmed with a constant heating rate of 10 °C/min.

2.3. Adsorption/desorption and surface reaction experiments

The adsorption/desorption and surface reaction of HCHO were performed in a fixed catalytic reactor system at the middle of which 0.1 g catalyst (20–40 mesh) was packed. The reaction was performed at temperatures ranged from room temperature (RT) to 500 °C. A thermocouple was placed in the middle of the catalyst bed for the temperature measurement. Gaseous HCHO was generated by flowing He over trioxymethylene (99.5%, Acros Organics) in an incubator kept in ice water mixture. A HCHO adsorption breakthrough curve was obtained for each run to ensure the saturation of the catalyst surface using the mass spectrum (Ametek, LC-D200M). The catalysts were purged with high purity helium for 1 h to fully remove physically adsorbed HCHO, and then the temperature was ramped at 10 °C/min from RT to 500 °C. The effluent from quartz reactor was analyzed by MS. The exhaust line from the reactor to the mass spectrometer was maintained at ~120 °C to prevent the condensation of the formaldehyde and reaction products.

Temperature programmed desorption (TPD) of HCHO was carried out in a continuous flow of helium, and the temperature

Table 1
BET, pore volume and pore diameter of the Ag/M catalysts (M: the different supports).

Samples	S_{BET} (m^2/g)	Pore volume (ml/g)	Pore diameter (nm)
NaY	544.9	0.4241	1.462
Ag/NaY	431.7	0.1055	1.423
SBA-15	482.3	0.6564	6.459
Ag/SBA-15	375.9	0.5917	5.941
MCM-41	538.8	0.6391	2.440
Ag/MCM-41	553.0	0.3852	2.188
SiO_2	245.4	0.3848	7.588
Ag/SiO_2	243.5	0.292	7.887
TiO_2	56.38	0.2922	17.805
Ag/TiO_2	29.12	0.1860	17.986

programmed surface reaction (TPSR) experiments were conducted in flow of O_2/Ar (30 vol.% O_2).

2.4. In situ FT-IR

In situ FT-IR spectra were recorded in BRUKER VERTEX 70 using variable-temperature quartz cells. A catalyst wafer (12 mm × 0.1 mm in size and ca. 30 mg in weight) was placed in the flow IR cell-reactor and then pretreated in He flow at 300 °C for 40 min. All spectra were recorded with a resolution of 4 cm^{-1} and accumulating 16 scans. A background spectrum was subtracted from each spectrum, respectively.

3. Results and discussion

3.1. Catalysts characterization

Table 1 lists the surface area (S_{BET}), mean pore diameters and total pore volume of different supports together with the silver based catalysts. It can be seen that the surface areas and pore volumes of the silver based catalysts are smaller than those of the pure supports. The small decrease of these parameters can be attributed to partial blockage of the porous materials by silver particles. However Ag/MCM-41 catalyst showed slightly higher surface areas (553 m^2/g) than that of pure support (538.8 m^2/g). It can be supposed that the Ag particles enter into that particular pore channels, resulting in the formation of new pore tunnel and displaying the few larger surface areas than the support. The pore size distribution of different silver based catalysts can be observed obviously in Fig. 1. Different silver catalysts showed different pore size distribution. Only microspores formed on the Ag/NaY, and Ag/TiO_2 had biggest pore size among all catalysts.

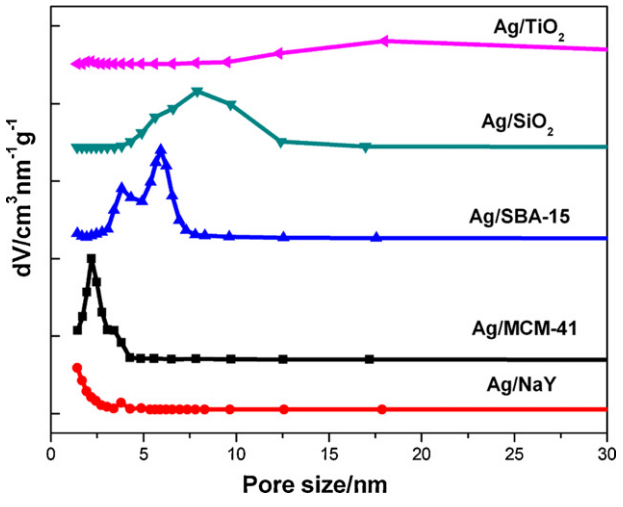

Fig. 1. Pore size distribution curves of Ag/M catalysts (M: the different supports).

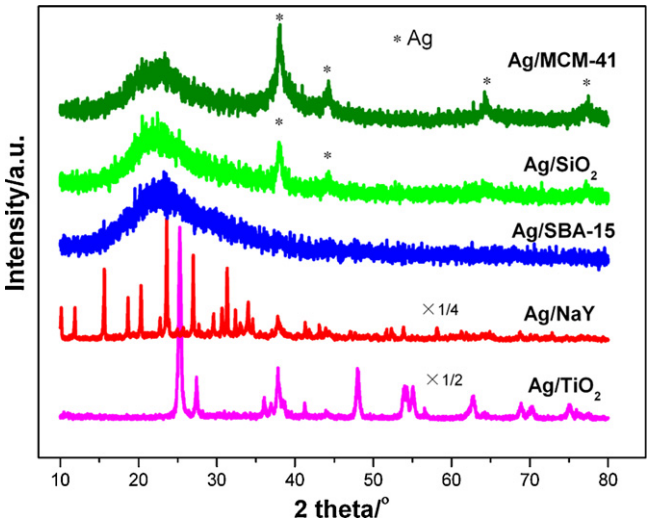

Fig. 2. XRD patterns of Ag/M catalysts.

Fig. 2 shows the XRD patterns of silver catalysts with different supports. For all the samples, no lines due to silver oxide were observed. For Ag/SBA-15, Ag/NaY and Ag/TiO_2 samples, the diffractions due to metallic silver particles were not observed clearly. Well dispersion of the silver particles on Ag/SBA-15 sample was obtained. The XRD peaks of Ag particles and the supports for the Ag/TiO_2, Ag/NaY samples overlap each other at 38°, so it is difficult to compare the Ag particle size based on the XRD results. An obvious diffraction peak for metallic silver at 2θ of 38.0° appeared for the Ag/MCM-41, Ag/SiO_2 samples, indicating the formation of the larger silver particles.

To elucidate the size and the dispersion of silver particles on the different support, TEM images and corresponding silver particles size distribution are shown in Fig. 3. The images are representative for the entire surface of the respective samples and show homogeneous distribution of the Ag nanoparticles on the support. For all the samples, the silver particles were between 2 and 10 nm in diameter. The Ag nanoparticles exhibited the excellent dispersion, and the average particle size was obviously larger for the Ag/MCM-41(d_m = 9.18 nm), Ag/SiO_2 (d_m = 8.45 nm) samples, whose result was similar to the result obtained from XRD. The size was smaller for Ag/SBA-15 (d_m = 5.58 nm) and Ag/NaY (d_m = 6.68 nm) catalysts, and it was clearly observed that the silver particles were well dispersed in the channels of the SBA-15 support from Fig. 3c. The silver particles seemed relatively small and little for Ag/TiO_2 sample (d_m = 3.80 nm).

It has been known the highly dispersed silver species could not be detected by XRD, and then the co-existence of various silver structures was further investigated by UV-Vis spectrometer. Fig. 4 shows the UV–Vis spectra of the selected silver based catalysts. These samples showed the similar bands and the appearance in the major peaks at 220, 280, and 410 nm was observed. The absorption bands around 220–230 nm which were assigned to the $4d^{10} \rightarrow 4d^9 5s^1$ transition of Ag^+ ions highly dispersed on the support [34,35] that were detected clearly in the spectra of Ag/NaY sample, which should be due to its strong ion exchange capacity for NaY support. Some small silver clusters ($Ag_n^{\delta+}$) gave rise to the absorption band of average intensity at 280 nm [36,37] in the spectra over Ag/NaY, Ag/TiO_2 and Ag/SiO_2 catalysts slightly. These silver clusters were consisted with several silver atoms, and could not be detected by XRD. The presence of the broad bands centered at 410 nm are the characteristic absorbance of metallic

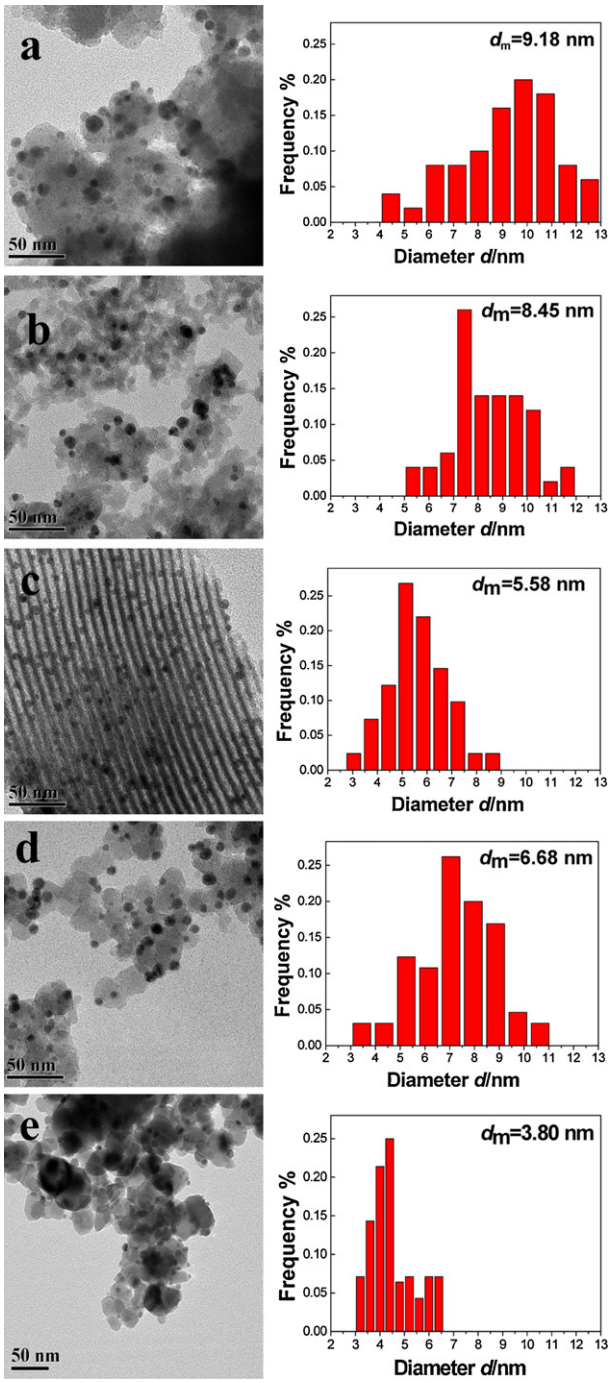

Fig. 3. TEM pictures of Ag/M catalysts (a: Ag/MCM-41, b: Ag/SiO_2, c: Ag/SBA-15, d: Ag/NaY, e: Ag/TiO_2).

silver particles, which may be several nanometers or much larger [35,38]. The absorption band at 410 nm was obviously observed on the Ag/MCM-41, Ag/SiO_2 samples, and the intense absorption band at 410 nm may be due to the highly dispersed silver particles for Ag/NaY catalyst, as shown in Fig. 3d. However no obvious absorption band at 410 nm was observed for Ag/TiO_2 sample.

Fig. 5 shows the H_2-TPR profiles of the corresponding Ag catalysts. A main peak (100–200 °C) in TPR profile was observed over all silver catalysts, and a broad reduction peak higher than 200 °C was also found for all samples except for Ag/TiO_2. The peak at around 100 °C in our experiments should be assigned as the well-dispersed silver oxides (below XRD detection limit) within the pore or on the

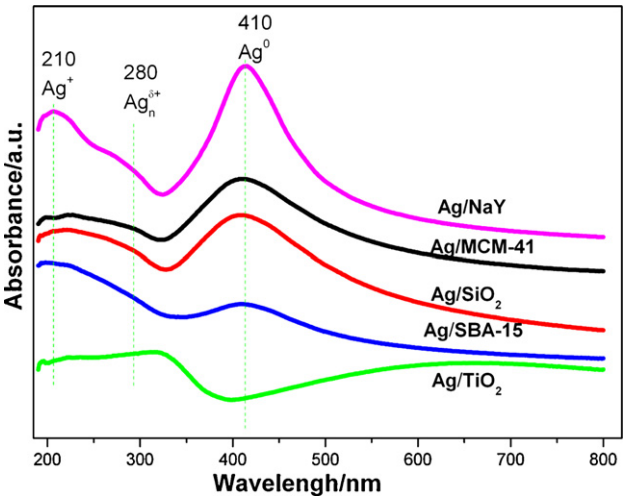

Fig. 4. UV–Vis spectra of Ag/M catalysts.

surface of sieves [26,39]. And the reduction peak temperature for dispersed silver oxides was related with the size of these species [36] and the similar phenomena was also observed, the reduction temperature moved to lower temperature with the increase of the silver loading. The detailed research will be discussed in our following paper. In addition, the high temperature reduction peak (above 600 °C) appeared over Ag/NaY catalyst, which was attributed to isolated Ag+ ions, as mentioned in UV–Vis results.

Interestingly, an obvious broad reduction peak higher than 200 °C was also found in H_2-TPR spectra for all silver catalysts expect for TiO_2 supported silver catalyst (Fig. 5). That is to say, some oxygen species in silver catalyst were slowly reduced in the studied temperature range. However no other silver-oxide species were observed from XRD and UV–Vis spectra. Shi et al. [40] have suggested that there exists amorphous character of ill-defined mixed silver oxides due to the broader absorption band at 430 nm even if no silver oxides and metallic silver was found in XRD during oxidative atmospheres pretreatment at high temperature over Ag-H-ZSM-5. No obvious similar absorption band for this kind of silver oxides was found in Fig. 4, which might be the coverage of strong broad absorption band of metallic silver or the existence of other oxygen species.

The interactions of silver with oxygen have been extensively studied in order to understand the catalytic behavior of silver cata-

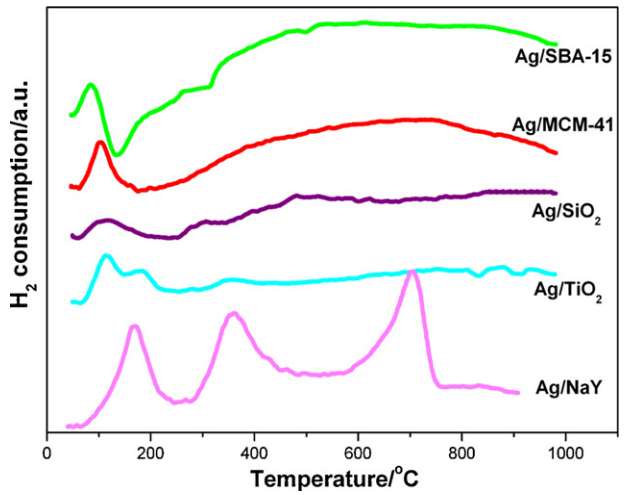

Fig. 5. H_2-TPR spectra of Ag/M catalysts.

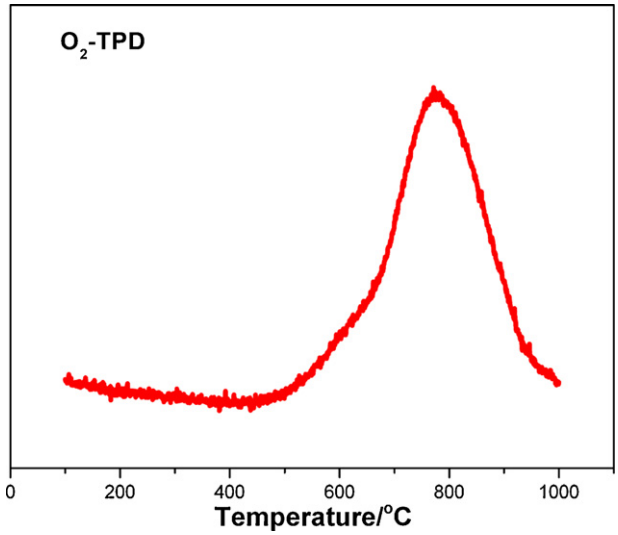

Fig. 6. O_2-TPD spectra of Ag/MCM-41 catalyst.

lysts. Various oxygen species have been observed on silver catalyst, for instance, the molecular, subsurface, and various forms of surface atomic oxygen by a variety of spectroscopic techniques, such as DFT, XPS, HRTEM, and O_2-TPD and so on [21,22,41]. O_2-TPD experiments have been used to study the interaction of the silver particles with oxygen and distinguish various oxygen species in our previous work [23]. Two oxygen desorption peaks appear in the TPD spectrum for the Ag/SiO_2 catalyst pretreated with oxygen at 500 °C. It is thought that the peak at the lower temperature is assigned to the bulk-oxygen species (O_β) and the desorption peak at higher temperatures (>600 °C) is attributed to subsurface oxygen (O_γ) [42–44]. In fact, the similar O_2 desorption peak was also observed for our silver catalysts in this work, as shown in Fig. 6. The similar oxygen desorption pattern was also observed on other silver catalysts except for the Ag/TiO_2 (not shown here). The subsurface oxygen species existed in the silver bulk after oxygen pretreatment at 500 °C for silver based catalysts. However the characteristics and the effect of the subsurface oxygen species on different supports were still not clear, which need the further study in the future. The amount of the subsurface oxygen species is gradually decreased with the hydrogen reduction from 50–500 °C [45]. Thus the broad reduction peak at higher than 200 °C in H_2-TPR profile should be due to the slow reduction of the subsurface oxygen species existed in the silver catalysts.

Therefore, it could be concluded that there exited the well-dispersed Ag_2O (below XRD detection limit), metallic Ag particles (Ag^0) with subsurface oxygen species, some isolated silver ions (Ag^+) and few $Ag_n^{\delta+}$ clusters in Ag based catalysts. The states, the dispersion and the amount of these silver species are obviously different on different supports. There were much more metallic Ag particles (Ag^0) (8–10 nm) with subsurface oxygen species and well-dispersed Ag_2O for Ag/MCM-41 and Ag/SiO_2 samples. Well dispersed Ag_2O, metallic Ag particles (Ag^0) with subsurface oxygen species, some isolated silver ions (Ag^+) and few $Ag_n^{\delta+}$ clusters existed on Ag/NaY. The Ag/SBA-15 sample possessed well dispersed Ag_2O, metallic Ag particles (Ag^0) (about 5 nm) with subsurface oxygen species. There were few well dispersed Ag_2O, metallic Ag particles (Ag^0) (about 3 nm), some $Ag_n^{\delta+}$ clusters on Ag/TiO_2.

3.2. Temperature programmed desorption (TPD) and temperature programmed surface reaction (TPSR)

All samples were pretreated in O_2/Ar (30 vol.% O_2) stream at 500 °C for 2 h before the experiments, and then the adsorption saturation of HCHO was executed. TPD and TPSR experiments were carried out in a continuous flow of He and O_2/Ar (30 vol.% O_2) atmosphere, respectively. Analysis of the desorbed species was done by mass spectrometry.

Fig. 7 shows the HCHO–TPD profiles of the different Ag/M and M (M: different support) samples. The HCHO adsorption–desorption performance on different Ag/M samples was firstly discussed. The desorption performance of HCHO on different silver based catalysts were different. One could directly see that Ag/MCM-41 catalyst showed the highest desorption capacity for HCHO in all silver catalysts. Three desorption peaks existed for all Ag catalysts after the curve-fitting procedure (not shown here). Ag/MCM-41 showed the strongest desorption ability for HCHO at low temperatures. The desorption temperature window was relative narrow for Ag/MCM-41 and Ag/SiO_2 samples, and the HCHO desorbed completely ended up with higher temperature for SBA-15 and NaY supported silver catalysts. The adsorbed amount was fewest for Ag/TiO_2 among all samples. It is all known that the porous materials have also adsorption capacity for HCHO. Moreover, the different supports show different adsorption characteristics. Thus the corresponding profiles of HCHO–TPD for parent supports are also shown for comparison purposes in Fig. 7 to elucidate the role of silver sites and support sites in the adsorption of formaldehyde. It was obviously observed that desorbed amount of HCHO decreased after silver loading for all samples, which should be partly due to the aggregation of the silver particles and the decrease of S_{BET} (Table 1). Compared with the parent support, an obvious new desorption peak for HCHO at low temperature appeared when silver was loaded on the MCM-41 and SiO_2 silica. The silver loaded on the

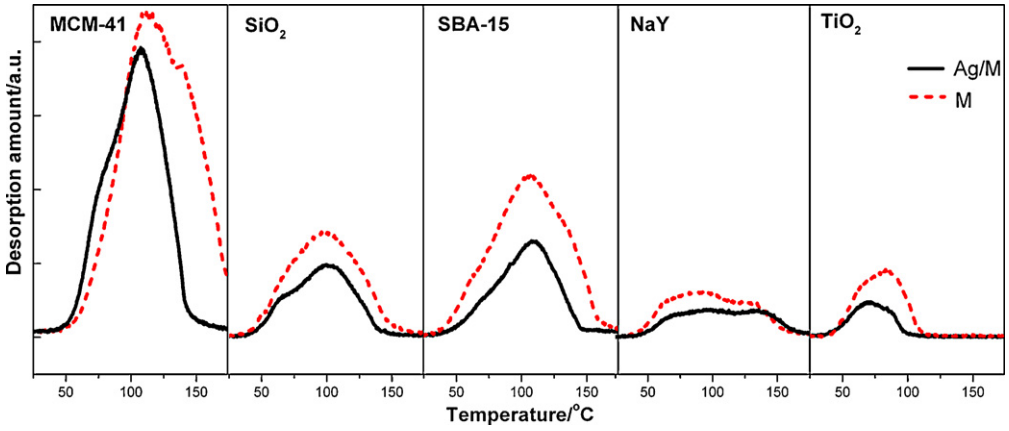

Fig. 7. HCHO–TPD profiles of different supports and supported silver catalysts.

MCM-41 and SiO_2 would provide new active adsorption sites for HCHO, which was easily desorbed at low temperature and more active. And the temperature window of formaldehyde desorption became narrower after silver loading. In the case of SBA-15 and NaY samples, it was indicated that a gradual shift of the HCHO desorption peak to higher temperature was accompanied by wide desorption temperature window. Moreover it was found that the ratio of the amount for third desorption peak (about 130 °C) with that of the second desorption peak (around 100 °C) increased when the silver loaded for the Ag/SBA-15 and Ag/NaY samples from the result of the curve-fitting. The shape of desorption profile and desorption window for HCHO had no significant changes for TiO_2 supported catalyst.

In our latest research [46], the size of silver particles played the key role in the low temperature HCHO desorption, only the metal silver particles with certain sizes exhibited the low temperature desorption for HCHO. The silver particles size over Ag/MCM-41 and Ag/SiO_2 was about 8–10 nm, whose size was very close to the size obtained in our previous result. Thus the metal silver particle with certain size was more prone to the adsorption of HCHO. The interaction of silver species with the adsorbed HCHO molecular became stronger as the size got too small for the Ag/SBA-15 and Ag/NaY samples, which resulted in the higher desorption temperature for HCHO.

Fig. 8A shows the TPSR results of silver catalyst pre-adsorbed HCHO on Ag/MCM-41 sample. It was found that O_2 was consumed and CO_2 and H_2O were produced eventually when the adsorbed HCHO reacted with the oxygen. The production of CO_2 ($m/e = 44$) means the reaction of adsorbed HCHO ($m/e = 30$) with O_2 ($m/e = 32$) at a certain temperature. The surface reaction activity of HCHO with oxygen on different silver based catalysts can be detected by inspecting the consumption of O_2. No O_2 consumption and CO_2 formation were observed on the pure supports during TPSR, thus the silver species was the active sites for the HCHO oxidation.

Fig. 8B shows the O_2-TPSR profiles of SiO_2, SBA-15, NaY, TiO_2 supported silver catalysts (only shown the oxygen profile). Different surface reaction activity of oxygen with adsorbed HCHO was observed on different silver based catalysts. Particularly, no O_2 consumption was observed for Ag/TiO_2 sample even at high temperatures (500 °C). As we all know, the reactant adsorption–desorption performances show strong influence on the catalytic activity of the catalysts. Usually, the lower desorption temperature for the active species, the higher catalytic activity at lower temperatures. The new adsorption sites for HCHO adsorption at low temperatures would promote the HCHO oxidation. The HCHO could be activated by oxygen at relatively low temperature (about 110°) for Ag/MCM-41 and Ag/SiO_2, and higher temperature for SBA-15 and NaY supported catalysts. This results were in agreement with the performance of HCHO desorption on different silver catalysts. The adsorbed HCHO desorbed at lower temperatures and was more active for oxidation on the MCM-41 and SiO_2 supported silver catalysts. The surface reaction for HCHO oxidation moved to higher temperature due to the broad HCHO desorption temperature window as smaller silver particles (<8 nm) formed on the SBA-15 and NaY supported silver catalysts.

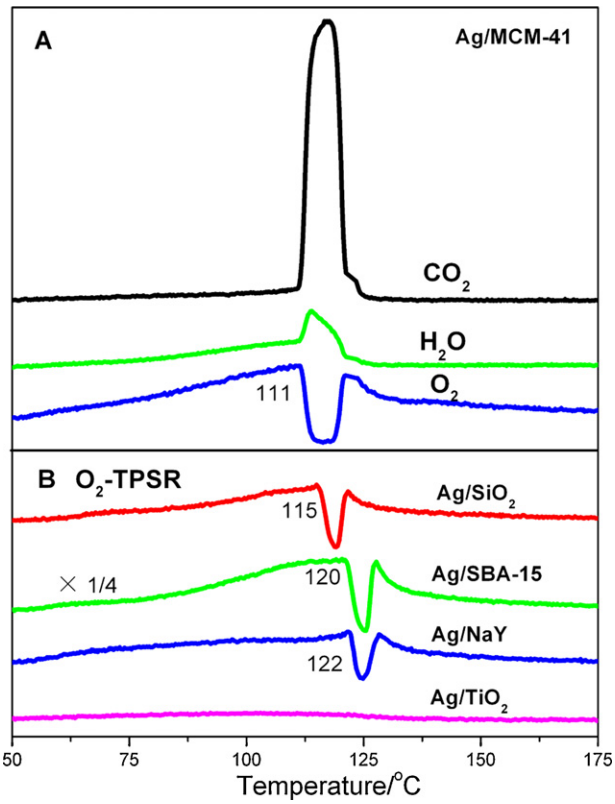

Fig. 8. TPSR profiles of Ag/MCM-41 catalyst (A) and O_2 consumption profiles (B) of Ag/SiO_2, Ag/SBA-15, Ag/NaY, and Ag/TiO_2.

It has been known that subsurface species are often been suggested to be responsible for the activation of catalyst surfaces for particular reaction [45,47–49], such as in activating oxygen for ethylene epoxidation [50] and for partial oxidation of methanol to formaldehyde [51] and in increasing the reaction probability for selective CO oxidation in the presence of H_2 [23]. The H_2

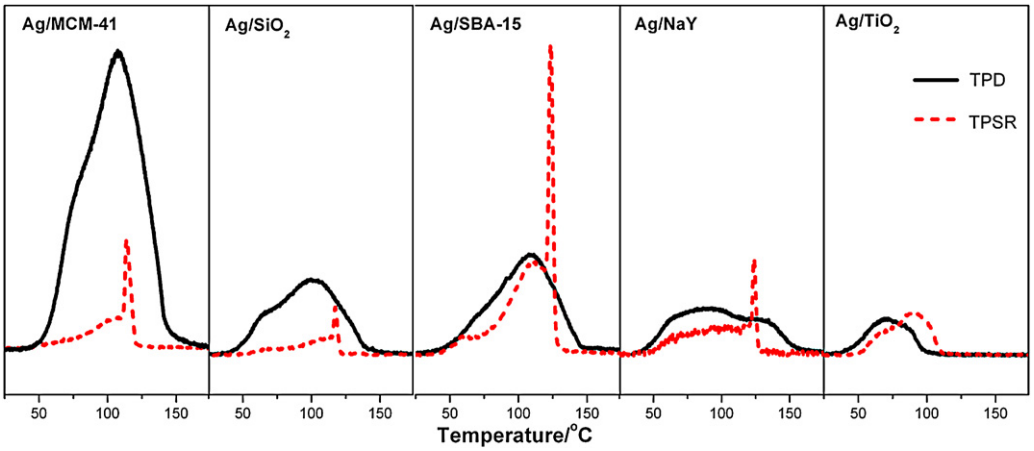

Fig. 9. HCHO-desorption spectra during TPD and TPSR experiments for Ag/M catalysts.

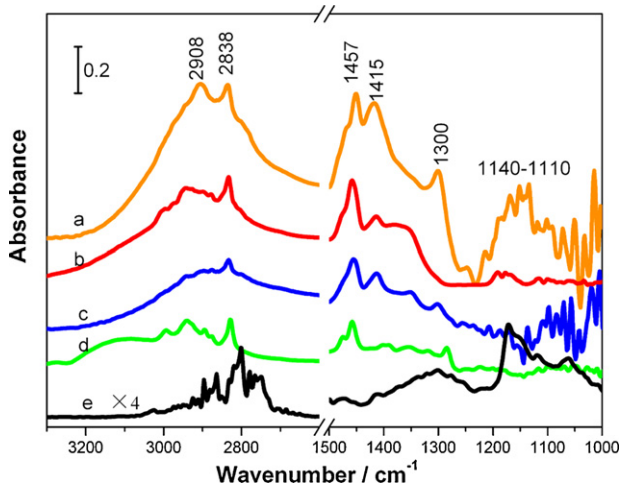

Fig. 10. FT-IR spectra of Ag/M catalysts after exposed to a flow of HCHO + He for 60 min (a: Ag/MCM-41, b: Ag/SiO_2, c: Ag/SBA-15, d: Ag/NaY, e: Ag/TiO_2).

reduction at high temperatures makes the disappearance of the subsurface oxygen and the aggregation of silver nanoparticles. In order to further investigate the effect of subsurface oxygen, the Ag/MCM-41 catalyst was reduced with H_2 at 500 °C and then to test its surface reaction activity for HCHO oxidation. No CO_2 formed during TPSR experiment (not shown here). Thus the existence of this kind of subsurface oxygen species in silver catalyst would be responsible for the HCHO adsorption and oxidation. We have found that amount of the subsurface oxygen species in the silver bulk would influence the adsorption and reaction of HCHO in our latest experiments.

The different desorption character for HCHO was also observed during TPSR process on different silver catalysts. Fig. 9 shows the HCHO desorption during TPD and TPSR process on the all samples. The desorption amount for HCHO sharply decreased during surface reaction compared with TPD patterns on Ag/MCM-41 and Ag/SiO_2 at low temperatures (50–100 °C). The initial temperature for the surface reaction of HCHO with oxygen was 111 °C and 115 °C, respectively, for the two samples. Thus it was believed that adsorbed HCHO was mostly dissociated to intermediate species (e.g., DOM or formate), resulting in the little desorption of the HCHO at low temperatures (<100 °C). However, the case seemed to be different for other samples. The results of HCHO desorption during TPD and TPSR process over Ag/SBA-15 and Ag/NaY are displayed in Fig. 9. There were still lots of adsorbed HCHO was desorbed at low temperatures during TPSR process, which enabled us to believe parts of the adsorbed HCHO was not dissociated to intermediates. The adsorbed HCHO adsorbed on the catalyst surface was desorbed into gas HCHO upon heating. Wang et al. [52] also found the similar results that the linear and the geminal CO absorbed on the catalyst surface did not dissociate, and only the tilt-adsorbed CO was the main precursor for CO dissociation. For TiO_2 supported silver catalyst, adsorbed HCHO was completely desorbed compared with that of pure support (Fig. 9), and meanwhile no HCHO was activated to react with oxygen (as shown in Fig. 8).

To well demonstrate the adsorption process, and detect the intermediate species formed on the surface of silver catalysts after HCHO adsorption, the in situ FT-IR experiments were conducted on support and supported silver catalysts. The adsorption and reaction over catalysts can be monitored by in situ FTIR spectroscopy, allowing the study of the adsorption as a function of time, temperature and tracing of each elementary reaction. Besides, the variations of the reactants and products and the appearance and disappearance of intermediate species can also be monitored by in situ FTIR. At present, many researches are supposed that there exists interme-

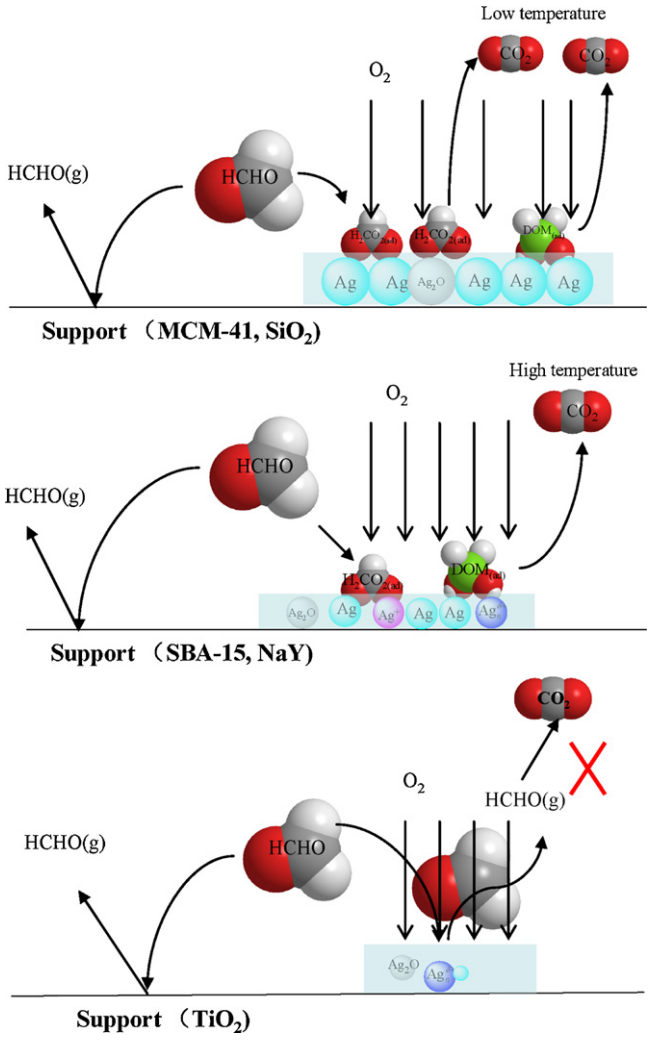

Fig. 11. Possible scheme for HCHO adsorption and surface oxidation to CO_2 on the surface of silver catalyst supported on different supports.

diate species such as dioxymethylene (DOM) or formate ions arising from the adsorption of HCHO [1,4,12], and the reaction activity is closely related with how much and how fast the formation of the intermediate species [12].

The samples were *ex situ* pretreated at 500 °C in O_2/Ar (30 vol.% O_2) for 2 h and followed by in situ pretreatment at 300 °C in He for 30 min before experiments. The adsorbed HCHO molecular (1720–1750 cm^{-1}) was observed in our FTIR experiments for Ag based catalysts during HCHO adsorption. Here we only discussed the formation of the intermediated species (DOM and formate ions) in Fig. 10 because the conversion of surface intermediates is the rate-determining step for the catalytic oxidation of HCHO [17]. The adsorption strength of the dioxymethylene (DOM) species at 1300 cm^{-1}, 1415 cm^{-1} and 1140 cm^{-1} and formate species at 2908 cm^{-1} [4,53] was obviously observed over silver catalysts after exposing the catalysts to HCHO + He mixture gas for 60 min at room temperature then purged by He for 60 min. The intensity of the DOM and formate species increased with the following order Ag/MCM-41 > Ag/SiO_2 > Ag/SBA-15 > Ag/NaY, which was consistent with the result of Fig. 9. Thus the surface reaction activity for HCHO oxidation over silver catalysts should be strongly related with the abilities of the formation of DOM and formate species. However, all of the intermediates were not reacted totally in HCHO oxidation. The intense HCHO oxidation was observed even though the less intermediates formed on Ag/SBA-15 sample. Therefore, the differ-

ent intermediate forms reacted as different mechanism, which will study in our next work.

Based on the discussion above, a simplified reaction scheme for the catalytic oxidation of HCHO on the different Ag based catalysts was postulated, as shown in Fig. 11. The silver based catalysts supported on the different supports showed different adsorption and reaction characteristics for HCHO, and the support played a key role on the state of the silver species on the support. The silver nanoparticles in certain size with some subsurface oxygen species gave new adsorption sites for HCHO, and facilitated its desorption at low temperatures. More intermediate species (DOM and formate) formed on the surface of the catalysts for Ag/MCM-41 and Ag/SiO_2 samples, thus resulting in the higher surface activity for HCHO oxidation. The higher desorption temperatures and its worse reaction performance should have connection with their few intermediate species formation on smaller Ag particles over SBA-15 and NaY supported silver catalysts. In contrast, the Ag/TiO_2 was not active for both the adsorption and the formation of intermediated species, and no activity for HCHO oxidation was observed.

4. Conclusions

In this work we investigated the formation of different silver species on different supports (silica, titania, NaY, MCM-41, SBA-15 zeolites) and their important roles in formaldehyde adsorption–desorption and surface reaction process. As indicated by XRD, UV–Vis and H_2-TPR, there were four kinds of silver species on the supports, including metallic Ag particles (Ag^0) with subsurface oxygen species, isolated Ag^+ ions, well dispersed Ag_2O and $Ag_n^{\delta+}$ clusters. The adsorption and reaction activity of HCHO was closed with the state of the silver species on the different supports. It was also found that the formation of subsurface oxygen after pretreatment was favor for HCHO oxidation. HCHO adsorbed on the silver sites was easily activated and desorbed at lower temperatures on the MCM-41 and SiO_2 supported silver catalysts, and the best activity for HCHO oxidation was obtained among the silver based catalysts. Ag/SBA-15 and Ag/NaY was less active for the activation and surface reaction of HCHO, and no activity for Ag/TiO_2 was found. It was also suggested that HCHO molecular adsorbed on silver sites was oxidized into dioxymethylene and formate surface species, and they reacted with oxygen to form CO_2 during TPSR. The surface reaction activity was strongly related with the formation of the DOM and formate species.

Acknowledgements

This work was supported financially by the National Nature Science Foundation of China (no. 20807010), the National High Technology Research and Development Program of China (863 Program) (no. 2009AA062604), the Specialized Research Fund for the Doctoral Program of Higher Education (no. 200801411111), the Program for New Century Excellent Talents in University (NCET-09-0256), the Program for Changjiang Scholars and Innovative Research Team in University (IRT0813) and the 123 Project of Liaoning environment education research supported by Geping Green finance for students.

References

[1] G. Busca, J. Lamotte, J.C. Lavalley, V. Lorenzelli, J. Am. Chem. Soc. 109 (1987) 5197.
[2] K.T. Chuang, B. Zhou, S. Tong, Ind. Eng. Chem. Res. 33 (1994) 1680.
[3] G.Y. Popova, T.V. Andrushkevich, Y.A. Chesalov, E.S. Stoyanov, Kinet. Catal. 41 (2000) 805.
[4] C.F. Mao, M.A. Vannice, J. Catal. 154 (1995) 230.
[5] Y.S. Xia, H.X. Dai, H.Y. Jiang, J.G. Deng, H. He, C.T. Au, Environ. Sci. Technol. 43 (2009) 8355.
[6] T.K. Tseng, H. Chu, H.H. Hsu, Environ. Sci. Technol. 37 (2003) 171.
[7] J.C.S. Wu, Z.A. Lin, F.M. Tsai, J.W. Pan, Catal. Today 63 (2000) 419.
[8] J. Tsou, P. Magnoux, M. Guisnet, J.J.M. Orfao, J.L. Figueiredo, Appl. Catal. B 57 (2005) 117.
[9] P. Lakshmanan, L. Delannoy, V. Richard, C. Methivier, C. Potvin, C. Louis, Appl. Catal. B 96 (2010) 117.
[10] S.C. Kim, W.G. Shim, Appl. Catal. B 92 (2009) 429.
[11] L. Delannoy, K. Fajerwerg, P. Lakshmanan, C. Potvin, C. Methivier, C. Louis, Appl. Catal. B 94 (2010) 117.
[12] C. Zhang, H. He, Catal. Today 126 (2007) 345.
[13] J. Peng, S. Wang, J. Phys. Chem. C 111 (2007) 9897.
[14] Y. Shen, X. Yang, Y. Wang, Y. Zhang, H. Zhu, L. Gao, M. Jia, Appl. Catal. B 79 (2008) 142.
[15] X. Tang, J. Chen, X. Huang, Y. Xu, W. Shen, Appl. Catal. B 81 (2008) 115.
[16] C. Zhang, H. He, K.-i. Tanaka, Appl. Catal. B 65 (2006) 37.
[17] X. Tang, J. Chen, Y. Li, Y. Li, Y. Xu, W. Shen, Chem. Eng. J. 118 (2006) 119.
[18] A. Montoya, B.S. Haynes, J. Phys. Chem. A 113 (2009) 8125.
[19] T. Kecskes, J. Rasko, J. Kiss, Appl. Catal. A 268 (2004) 9.
[20] A.K. Datye, D.J. Smith, Catal. Rev.-Sci. Eng. 34 (1992) 129.
[21] X. Bao, M. Muhler, B. Pettinger, R. Schlogl, G. Ertl, Catal. Lett. 22 (1993) 215.
[22] X. Bao, M. Muhler, R. Schlogl, G. Ertl, Catal. Lett. 32 (1995) 185.
[23] Z.P. Qu, M.J. Cheng, W.X. Huang, X.H. Bao, J. Catal. 229 (2005) 446.
[24] D. Tian, G.P. Yong, Y. Dai, X.Y. Yan, S.M. Liu, Catal. Lett. 130 (2009) 211.
[25] F. Bertinchamps, C. Gregoire, E.M. Gaigneaux, Appl. Catal. B 66 (2006) 1.
[26] S.-W. Baek, J.-R. Kim, S.-K. Ihm, Catal. Today 93–95 (2004) 575.
[27] C. He, J.J. Li, J. Cheng, L.D. Li, P. Li, Z.P. Hao, Z.P. Xu, Ind. Eng. Chem. Res. 48 (2009) 6930.
[28] R.H. Wang, J.H. Li, Catal. Lett. 131 (2009) 500.
[29] C. Li, Y. Shen, M. Jia, S. Sheng, M.O. Adebajo, H. Zhu, Catal. Commun. 9 (2008) 355.
[30] D.E. De Vos, M. Dams, B.F. Sels, P.A. Jacobs, Chem. Rev. 102 (2002) 3615.
[31] M. Boutros, J.M. Trichard, P. Da Costa, Appl. Catal. B 91 (2009) 640.
[32] R.Q. Long, R.T. Yang, J. Catal. 198 (2001) 20.
[33] X. She, M. Flytzani-Stephanopoulos, J. Catal. 237 (2006) 79.
[34] Z. Li, A. Chou, F.-M. Tao, Chem. Phys. Lett. 313 (1999) 313.
[35] A. Keshavaraja, X. She, M. Flytzani-Stephanopoulos, Appl. Catal. B 27 (2000) L1.
[36] K.A. Bethke, H.H. Kung, J. Catal. 172 (1997) 93.
[37] K.-i. Shimizu, J. Shibata, H. Yoshida, A. Satsuma, T. Hattori, Appl. Catal. B 30 (2001) 151.
[38] L. Kundakovic, M. Flytzani-Stephanopoulos, Appl. Catal. A 183 (1999) 35.
[39] T. Furusawa, K. Seshan, J.A. Lercher, L. Lefferts, K.-i. Aika, Appl. Catal. B 37 (2002) 205.
[40] C. Shi, M.J. Cheng, Z.P. Qu, X.H. Bao, J. Mol. Catal. A 235 (2005) 35.
[41] D.S. Su, T. Jacob, T.W. Hansen, D. Wang, R. Schlogl, B. Freitag, S. Kujawa, Angew. Chem. Int. Ed. 47 (2008) 5005.
[42] D.I. Kondarides, X.E. Verykios, J. Catal. 158 (1996) 363.
[43] X. Bao, M. Muhler, T. Schedel-Niedrig, R. Schll, Phys. Rev. B 54 (1996) 2249.
[44] D. Herein, A. Nagy, H. Schubert, G. Weinberg, E. Kitzelmann, R. Schlogl, Z. Physik. Chem. Int. J. Res. Phys. Chem. Chem. Phys. 197 (1996) 67.
[45] Z.P. Qu, W.X. Huang, M.J. Cheng, X.H. Bao, J. Phys. Chem. B 109 (2005) 15842.
[46] D. Chen, Z. Qu, W. Zhang, X. Li, Q. Zhao, Y. Shi, Colloids Surf. A: Physicochem. Eng. Aspects 379 (2011) 136.
[47] L. Gang, B.G. Anderson, J. van Grondelle, R.A. van Santen, Appl. Catal. B 40 (2003) 101.
[48] J. Hohmeyer, E.V. Kondratenko, M. Bron, J. Krohnert, F.C. Jentoft, R. Schlogl, P. Claus, J. Catal. 269 (2010) 5.
[49] A.B. Mohammad, I.V. Yudanov, K.H. Lim, K.M. Neyman, N. Rosch, J. Phys. Chem. C 112 (2008) 1628.
[50] J.G. Serafin, A.C. Liu, S.R. Seyedmonir, J. Mol. Catal. A 131 (1998) 157.
[51] A.J. Nagy, G. Mestl, R. Schlogl, J. Catal. 188 (1999) 58.
[52] Y. Wang, H.Y. Luo, D.B. Liang, X.H. Bao, J. Catal. 196 (2000) 46.
[53] T. Kecskes, J. Rasko, J. Kiss, Appl. Catal. A 273 (2004) 55.